High Temperature Thick Film Sensor Development Based on Refractory Oxide Semiconductors

Javier A. Mena[1], Katarzyna Sabolsky[1], Anthony A. Abrahamian[1], Domenic T. Cipollone[1], Konstantinos Sierros[1], **Edward M. Sabolsky[1]**, Víctor Mendoza-Estrada[2]

[1]Department of Mechanical and Aerospace Engineering,
West Virginia University, Morgantown, WV 26506, USA

[2]Applied Physics Research Group, Physics Department,
Universidad del Norte, Barranquilla, Colombia

ICMSN- 22
London, UK
July 12-14, 2022

WestVirginiaUniversity.

Introduction

- Processes such as energy generation, metals/glass manufacturing, coal gasification and aerospace technology applications require health and process monitoring in harsh-environments.
- **Harsh-environments conditions include:**
  - ❖ High temperature (500-1800^{o}C)
  - ❖ High pressure (up to 1000 psi)
  - ❖ Corrosive, erosive and reducing environments.
- **Ability to monitor:**
  - ❖ Temperature
  - ❖ Structural stability of systems components

- **US DOE Overall Goal:** Develop health and temperature sensors (and sensor arrays) printed on refractory produced by advanced 2D/3D printing.

Objectives of This Work

1) Synthesize high-temperature refractory $LaCrO_3$ powders with various p-type doping schemes using the Pechini sol-gel method.

2) Characterization phase development/structure (XRD), microstructure and grain size distribution (SEM), optical properties (UV-Vis) and bulk density.

3) Study the electrical properties (electrical conductivity and Seebeck coefficient) of compositions at high temperatures conditions and various atmospheres (oxidizing, reducing, different oxygen partial pressures) of these compositions.

4) Computational DFT modeling of the $LaCrO_3$ structure and electrical properties.

5) Fabricate surface printed thick-film temperature sensors utilizing these materials and test at high-temperature.

Lanthanum Chromite: General Aspects

- High melting point (~2500 °C).
- Chemically stable under oxidative and reducing atmospheres.
- Pure $LaCrO_3$ shows semiconducting behavior with no to low ionic conduction.
- σ = >10-100 $S \cdot cm^{-1}$ (RT – 1000°C).
- Compatibility (thermal expansion coefficients matching) near refractory materials, ~10×10^{-6} C^{-1}).

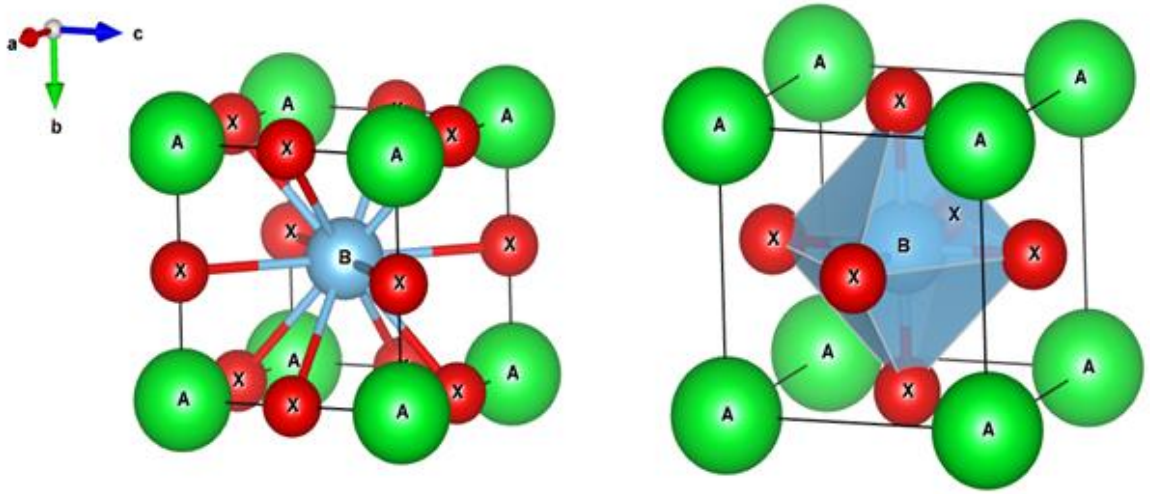

A atom cubic unit cell *B atom cubic unit cell*

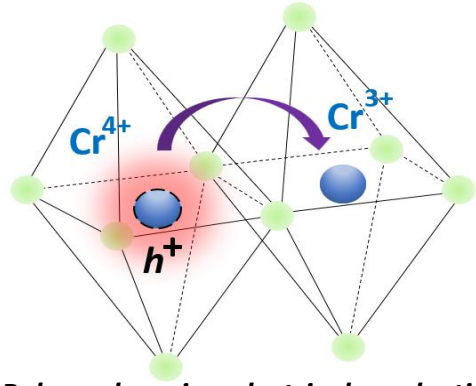

Polaron hopping electrical conduction

***Electrical properties (mostly in the 1990-2000's) in literature typically shown for <1000°C due to original focus for Solid-Oxide Fuel Cell (SOFC) applications.**

Sol Gel Synthesis and Pellet Fabrication

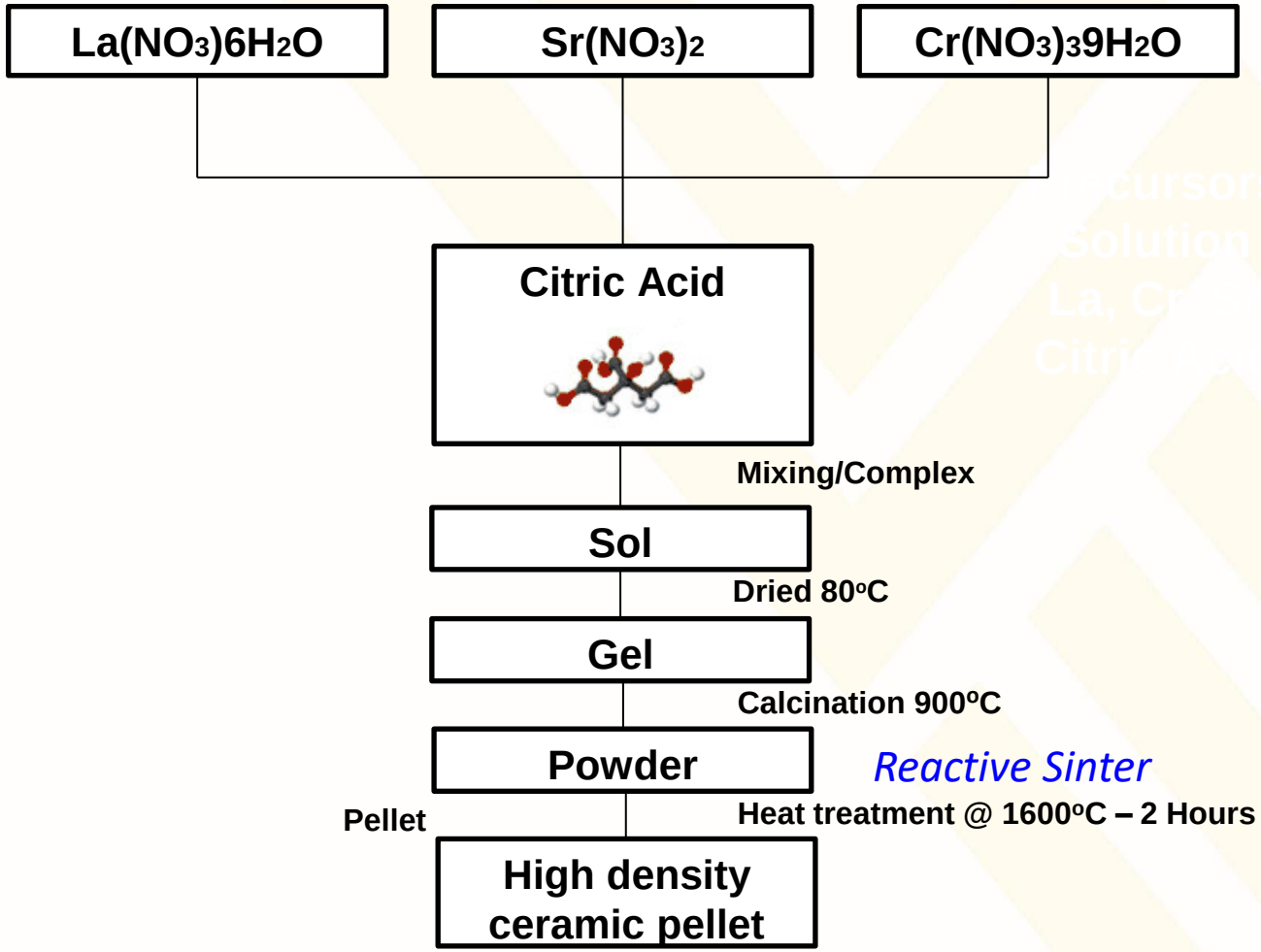

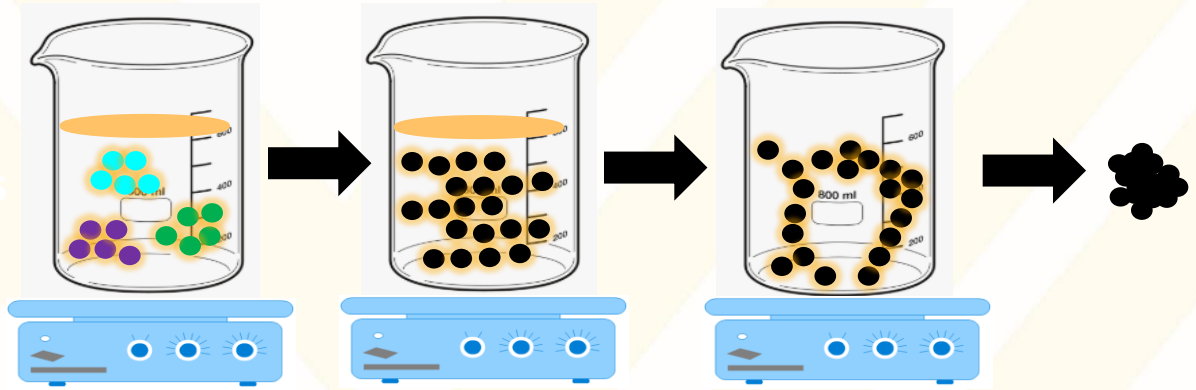

- ✓ Pechini-like process used.
- ✓ High homogenous and adequate sintering.
- ✓ High density (typical in literature <93% density).
- ✓ Low yields and not easy to scale-up

Compositions Studied:

A-site: $La_{1-x}\mathbf{Sr}_xCrO_3$, $La_{1-x}\mathbf{Ca}_xCrO_3$

(x = 0, 0.1, 0.2, 0.4)

B-site: $La_{0.8}Sr_{0.2}Cr_{1-y}\mathbf{Mn}_yO_3$

(y = 0, 0.1, 0.2, 0.4)

Crystalline Structure/Phase Analysis

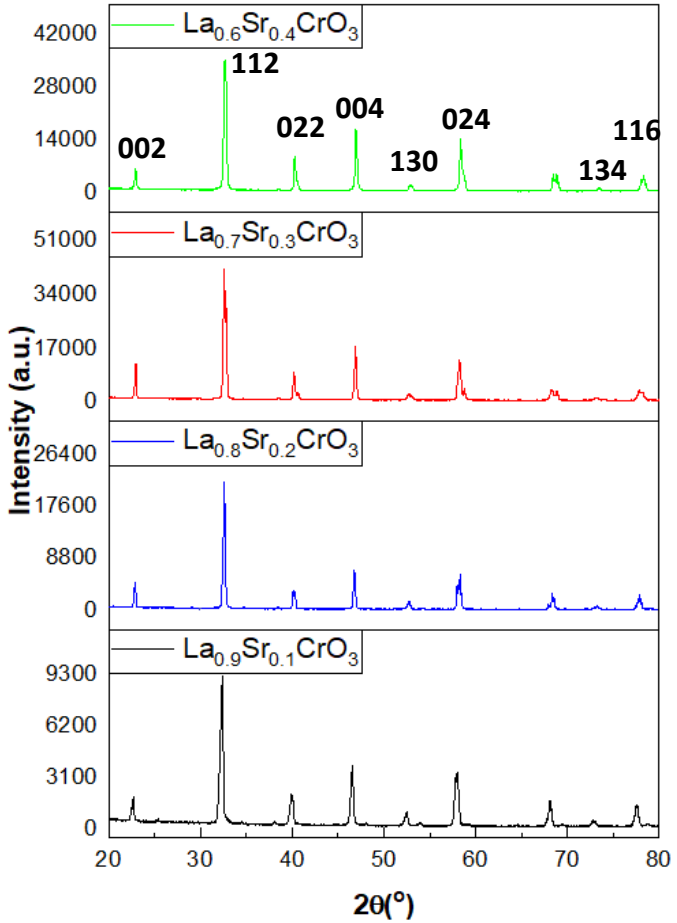

X-ray diffractograms for the samples of the $La_{1-x}Sr_xCrO_3$ series

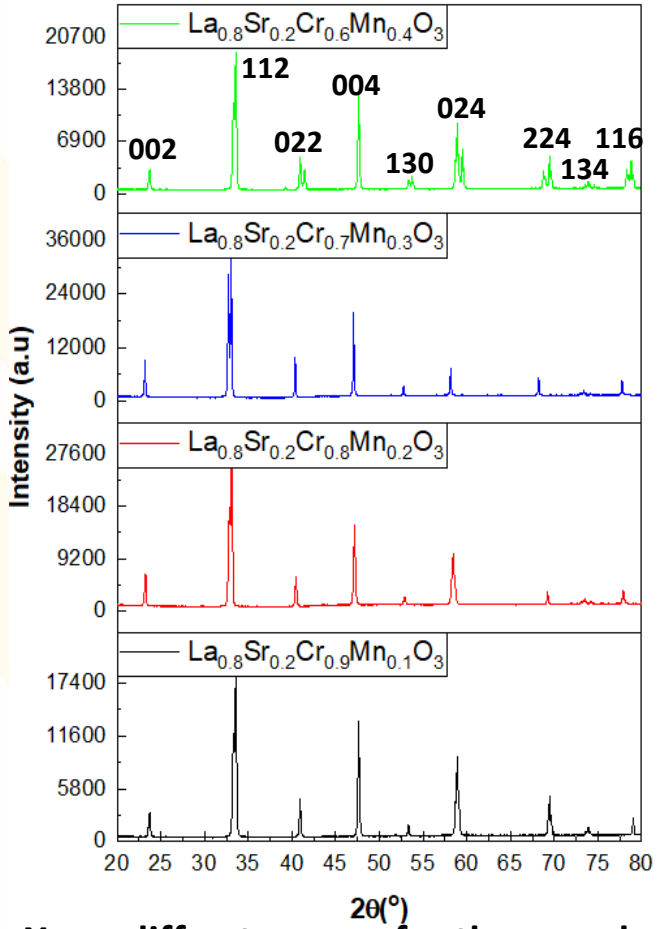

X-ray diffractograms for the samples of the $La_{1-x}Sr_xCr_{1-y}Mn_yO_3$ series

- Single phase doped lanthanum chromites materials were obtained successful (no residual oxide or pyrochlore peaks).
- Using Pechini Sol-Gel method permitted doped lanthanum chromites at high solubility levels (40%).
- No impurities extra peaks were present in the final prepared powders and ceramic pellets.

Lattice Parameters, Unit Cell Volume and Density

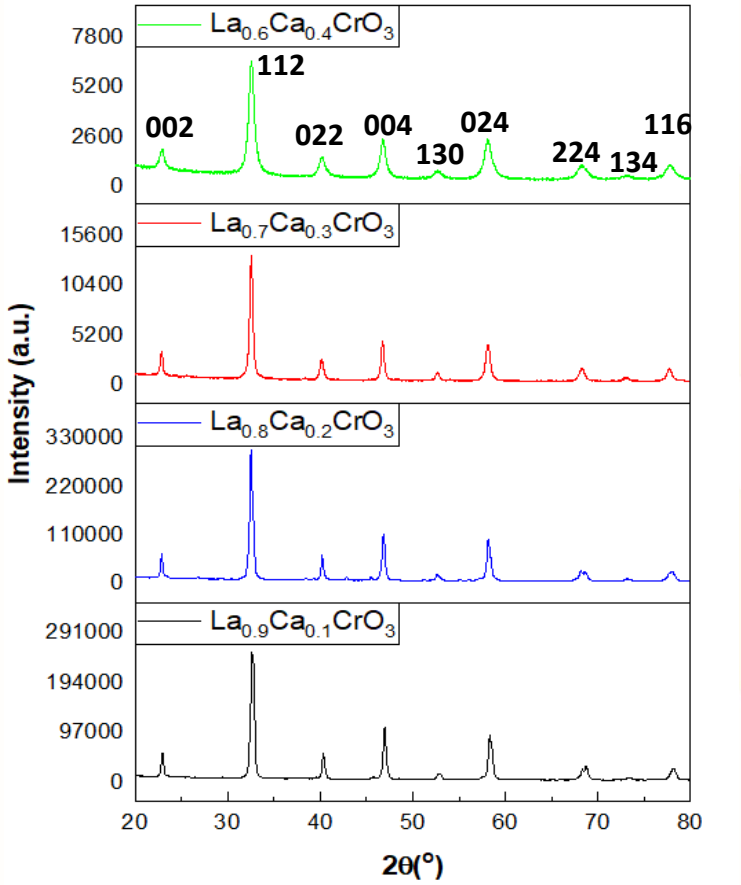

X-ray diffractograms for the samples of the $La_{1-x}Ca_xCrO_3$ series

%Sr↑

%Ca↑

%Mn↑

Lattice parameters, unit cell volume and XRD theoretical density for doped lanthanum chromites perovskites

Composition	Lattice parameters (Å)			Volume ($Å^3$)	$\rho XRD_{Theoretical}$ (g/cm^3)
	a	b	c		
$La_{0.9}Sr_{0.1}CrO_3$	5.5124	5.5668	7.7926	239.1299	6.4932
$La_{0.8}Sr_{0.2}CrO_3$	5.4988	5.5425	7.7853	237.2747	6.4004
$La_{0.7}Sr_{0.3}CrO_3$	5.4769	5.5233	7.7580	234.6839	6.3259
$La_{0.6}Sr_{0.4}CrO_3$	5.4524	5.5122	7.7407	232.6441	6.2350
$La_{0.9}Ca_{0.1}CrO_3$	5.4180	5.5039	7.7332	230.6050	6.5963
$La_{0.8}Ca_{0.2}CrO_3$	5.4092	5.4982	7.7264	229.7898	6.3341
$La_{0.7}Ca_{0.3}CrO_3$	5.3994	5.4877	7.7058	228.3264	6.0872
$La_{0.6}Ca_{0.4}CrO_3$	5.3897	5.4622	7.6853	226.2520	5.8528
$La_{0.8}Sr_{0.20}Cr_{0.90}Mn_{0.10}O_3$	5.4734	5.5648	7.7765	236.8595	6.1533
$La_{0.8}Sr_{0.20}Cr_{0.80}Mn_{0.20}O_3$	5.4705	5.5587	7.7702	236.2829	6.1766
$La_{0.8}Sr_{0.20}Cr_{0.70}Mn_{0.30}O_3$	5.4598	5.5398	7.7498	234.4020	6.2344
$La_{0.8}Sr_{0.20}Cr_{0.60}Mn_{0.40}O_3$	5.4146	5.4981	7.7065	229.4225	6.3783

- Decrease in lattice parameters (and volume) were observed when dopant cations is introduced in the lattice.
- To achieve neutrality chromium oxidation states, change from Cr^{+3} to Cr^{+4}, reduction in the chromium ionic size occurs.

Microstructure/Grain Size Distribution

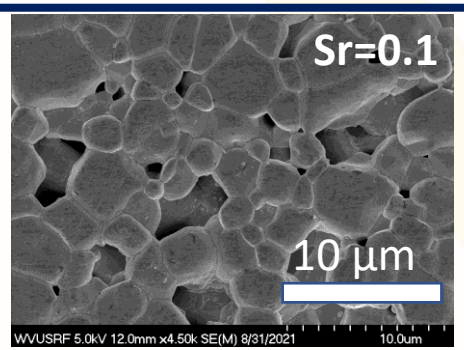

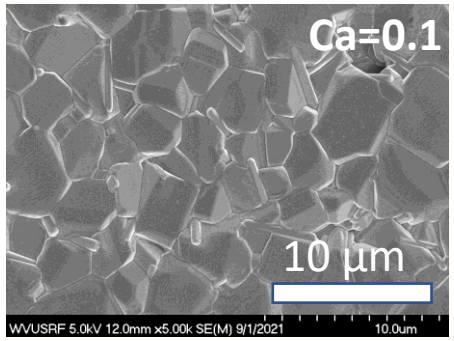

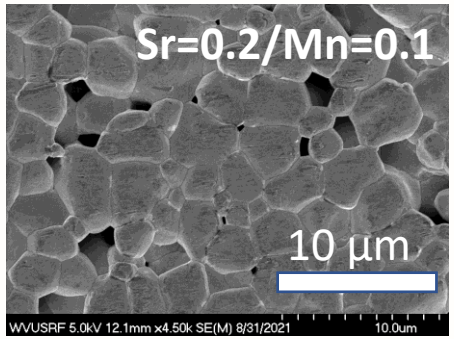

Average grain size and bulk density distribution for $La_{1-x}Sr_xCrO_3$, $La_{1-x}Ca_xCrO_3$, $La_{1-x}Sr_xCr_{1-y}Mn_yO_3$ series

Composition	Average Grain Size (µm)	Relative Percentage Bulk Density (%)
$La_{0.9}Sr_{0.1}CrO_3$	3.6480	94
$La_{0.8}Sr_{0.2}CrO_3$	3.4898	95
$La_{0.7}Sr_{0.3}CrO_3$	3.6290	95
$La_{0.6}Sr_{0.4}CrO_3$	3.2455	94
$La_{0.9}Ca_{0.1}CrO_3$	4.1367	96
$La_{0.8}Ca_{0.2}CrO_3$	3.7727	97
$La_{0.7}Ca_{0.3}CrO_3$	3.6883	97
$La_{0.6}Ca_{0.4}CrO_3$	3.6548	98

%Sr↑

%Ca↑

- Pechini Sol Gel prepared calcium, strontium, manganese doped lanthanum chromite powders exhibit better sinterability and densification under oxidizing conditions (undoped ↓90%).
- The samples of Ca doped lanthanum chromite powder have more dense microstructures. Furthermore, it was found that the incorporation of Ca, Sr in the A site of the lanthanum chromite increases grain growth (undoped <3 µm).

DC Electrical Conductivity (Oxidizing Atmosphere)

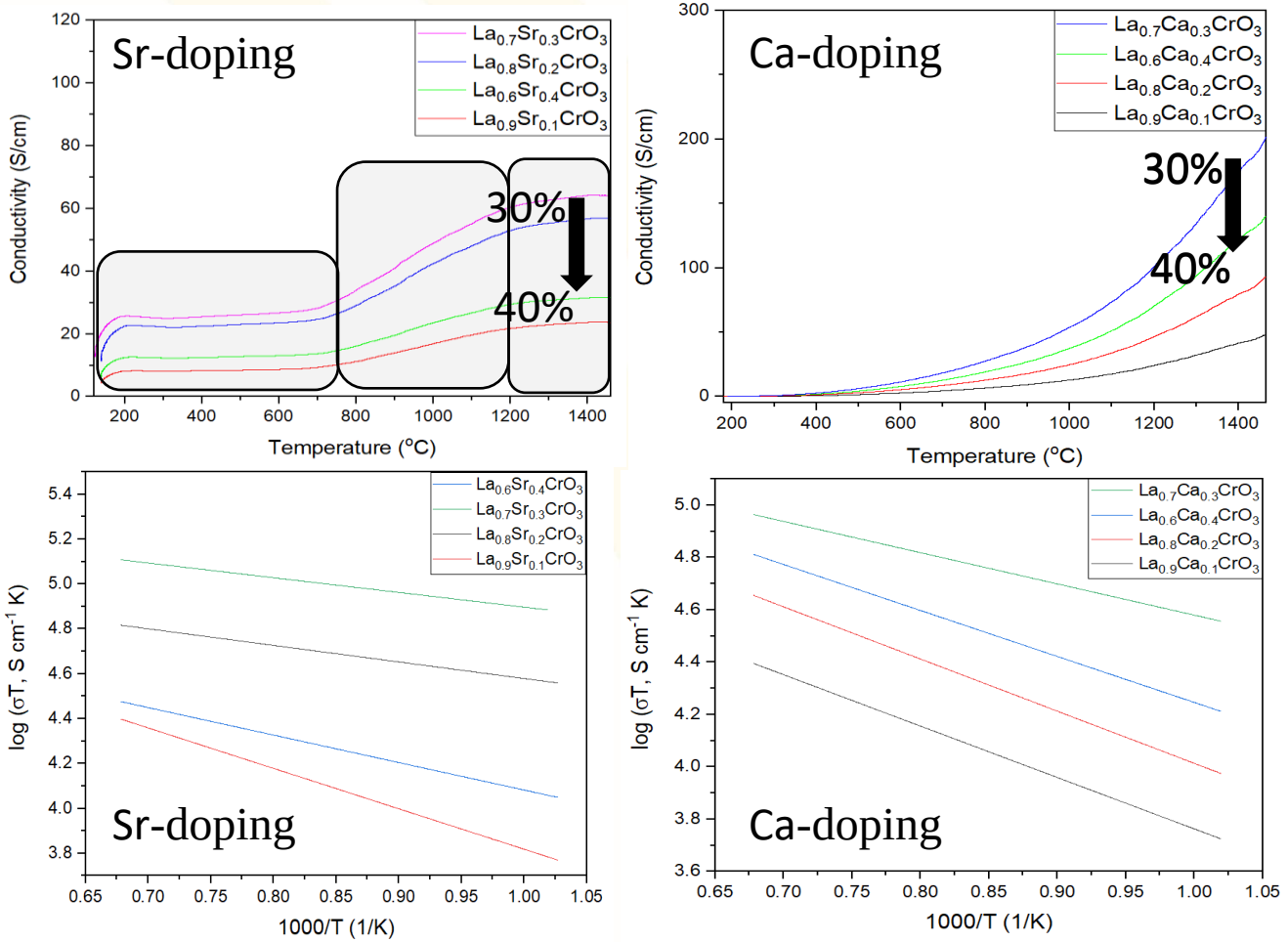

Electrical conductivity vs temperature and Arrhenius Plot $La_{1-x}Sr_xCrO_3$, $La_{1-x}Ca_xCrO_3$

- Conductivity typically exponentially increases with increase in carrier mobility, but 30 to 40% all drop in conductivity (believe slight second phase or higher lattice strain).
- Sr doped shows three regions, not seen in literature, since most tests <850°-1000°C. (believe V_o at high temperature)
- Arrhenius relationship fits for higher temperature regimes.
- Calcium doped compositions present higher conductivity due the lower distortion effects on lattice structure.

DC Electrical Conductivity (Reducing Atmosphere)

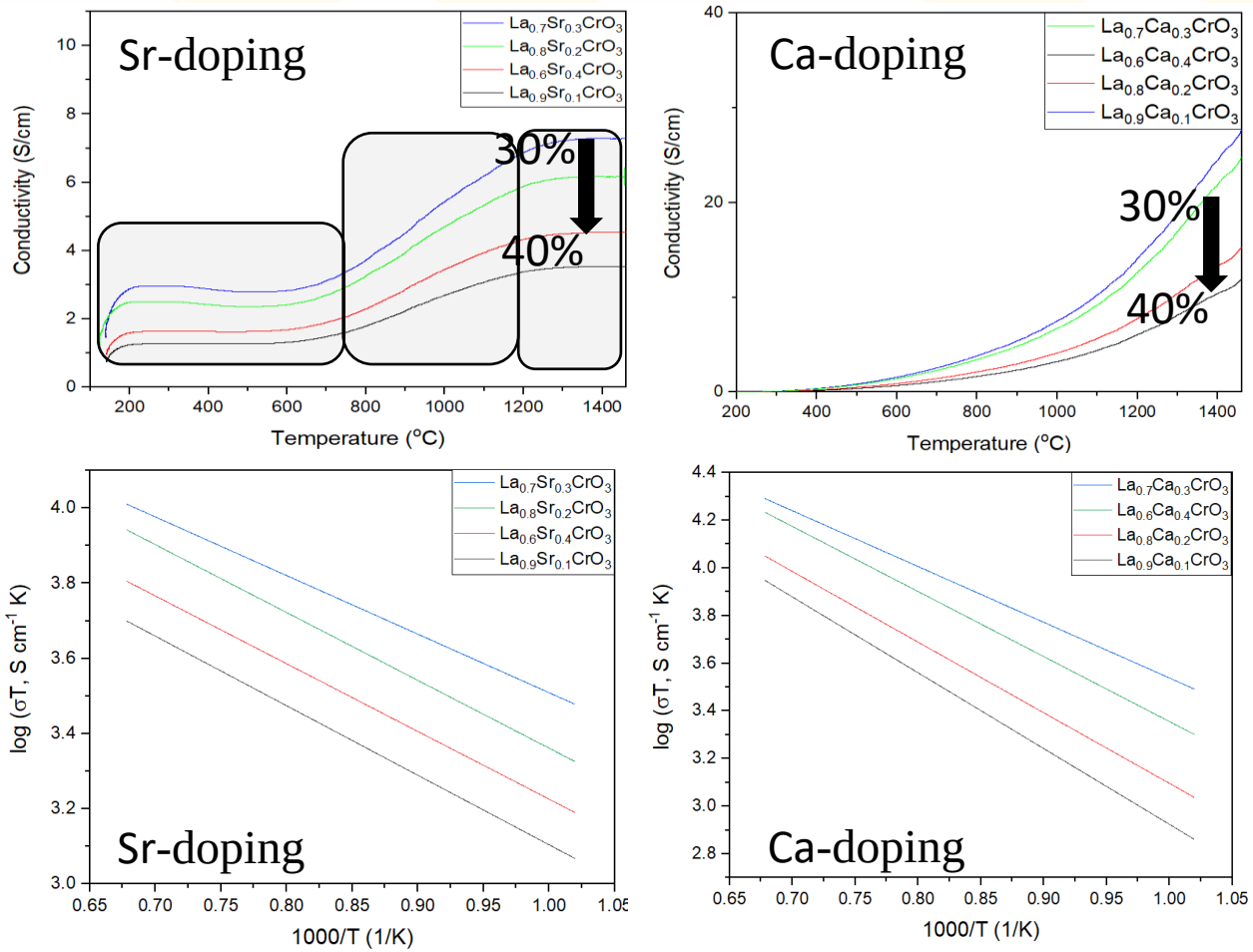

Electrical conductivity vs temperature and Arrhenius Plot for $La_{1-x}Sr_xCrO_3$, $La_{1-x}Ca_xCrO_3$

- Conductivity decrease for all temperature range under reducing atmosphere (H_2 5%/ N_2 95%).
- Under reducing conditions, oxygen vacancies form to keep neutrality (drop in hole carrier concentration).
- Sr conductivity still displays regions of altered mechanism.
- All compositions present lower conductivity as dopant increases (but still 40% lower than 30% in all cases).

DC Electrical Conductivities/Activation Energies

Composition	Air Atmosphere		Reducing Atmosphere	
	Conductivity @ 1000°C (S/cm)	Activation energy (eV)	Conductivity @ 1000°C (S/cm)	Activation energy (eV)
$La_{0.9}Sr_{0.1}CrO_3$	16.672	0.1552	2.691	0.3238
$La_{0.8}Sr_{0.2}CrO_3$	42.882	0.1427	4.572	0.2597
$La_{0.7}Sr_{0.3}CrO_3$	49.032	0.1055	5.534	0.1719
$La_{0.6}Sr_{0.4}CrO_3$	23.599	0.1498	3.462	0.3102
$La_{0.9}Ca_{0.1}CrO_3$	13.211	0.1417	3.152	0.3240
$La_{0.8}Ca_{0.2}CrO_3$	24.170	0.1298	4.118	0.2103
$La_{0.7}Ca_{0.3}CrO_3$	52.823	0.1028	7.602	0.1367
$La_{0.6}Ca_{0.4}CrO_3$	38.152	0.1175	6.626	0.1747

$$\sigma = \frac{\sigma_0}{T}\exp\left(\frac{-\Delta E_a}{kT}\right)$$

Slope $\propto E_a$

- Conductivity increase as function of doping level up to 30% for all dopants (strontium, calcium and manganese).
- At 40% doping levels conductivity decrease due to higher lattice distortion in all systems (solubility limit).
- Calcium and strontium/manganese doping obeys Arrhenius exponential law.
- Lower conductivity values under reducing atmospheres are explained by oxygen vacancies formation (near >1.5× in activation energy).

Computational Modelling for Ca-Doping Compositions

- First-principles spin-polarized calculation within the density functional theory (DFT) framework were performed.
- Exchange and correlation effects were treated with generalized gradient approximation (GGA) and GGA+U method implemented in the Perdew-Burke-Ernzerhof functional (PBE). Vienna Ab initio Simulation Package (VASP) was used.
- A cutoff energy of 520 eV, and a 3×6×4 k-point mesh was employed for a $2a \times 1b \times 1c$ $LaCrO_3$ orthorhombic supercell.
- The transport properties such as electrical conductivity (σ) was calculated using the BoltzTraP2 code that is formulated according to classical Boltzmann transport equation under the constant relaxation time (τ) approximation (σ can only be obtained in units of τ, since there is no experimental data available on the relaxation time in this material).

Work by: Victor Julio Mendoza Estrada (at Universidad del Norte)
Email: evictor@uninorte.edu.co

DFT and Experimental Lattice Parameters

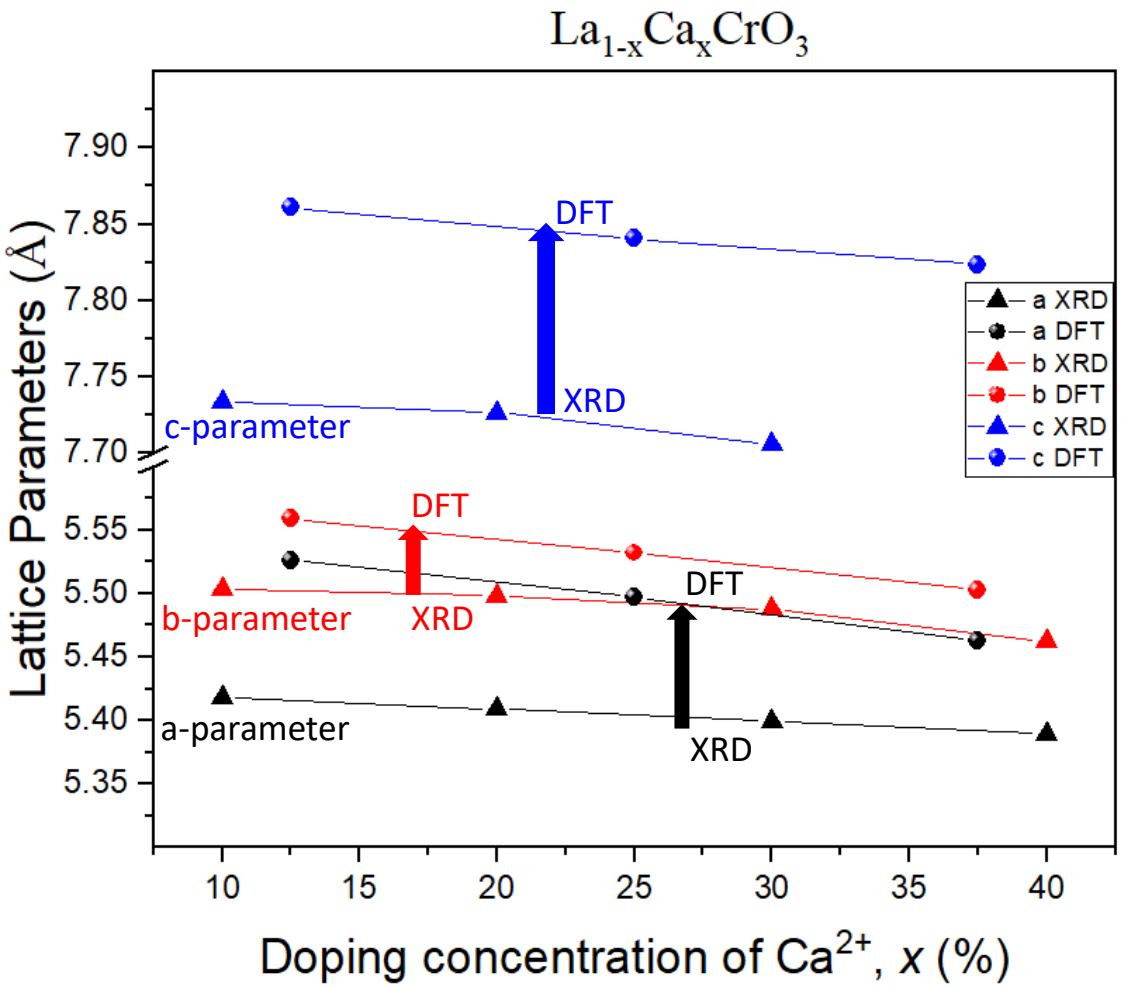

- Decrease in lattice parameters were observed when dopant cations is introduced in the lattice.
- To achieve neutrality chromium oxidation states, change from Cr^{+3} to Cr^{+4}, reduction in the chromium ionic size occurs.
- DFT theoretical data shows equal trends in the correlation between dopant level and lattice parameters as experimental data.
- DFT calculations of lattice parameters over-estimates lattice parameters values for all dopants and compositions in contrast with experimental XRD measurements.

Calculated Electrical Conductivity for Ca-Doping

DFT Results

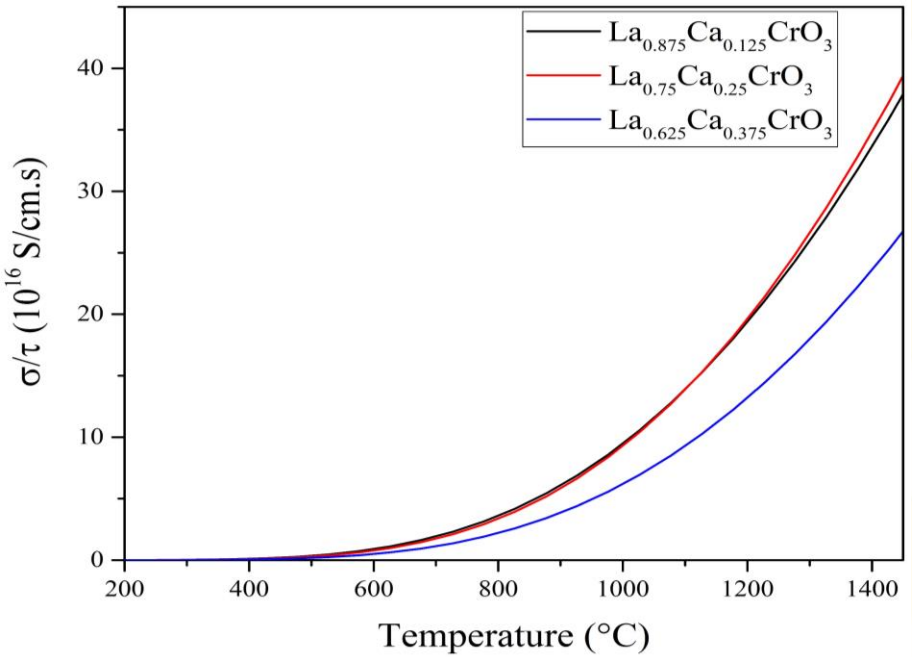

Experimental Results

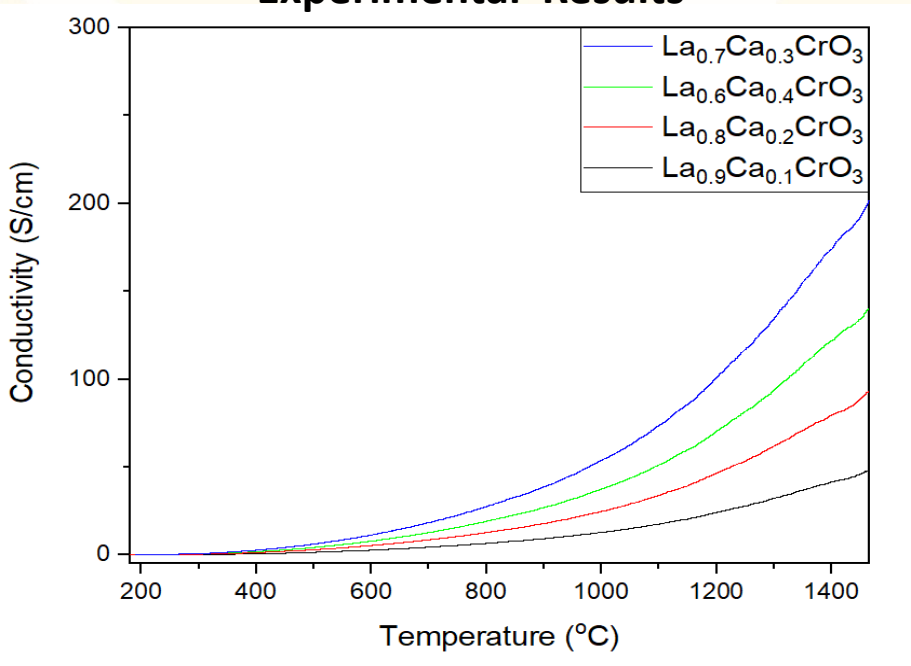

- The Ca-doped electrical conductivity presents proportional correlation increment with temperature, which is agreement with our experimental results.
- DFT calculated conductivity increase as a function of doping level up to 25% for calcium doping.
- DFT differ from experimental where 25-37.5% show similar conductivity, but not shown for experimental.

High Temperature Thermocouple Fabrication

- Research team currently fabricating strain, spallation, failure, thermistors and thermocouples by Direct Ink Writing (DIW) 3D printing.
- High-temperature thermocouples that function >1200°C (in R-type range) new exciting development.

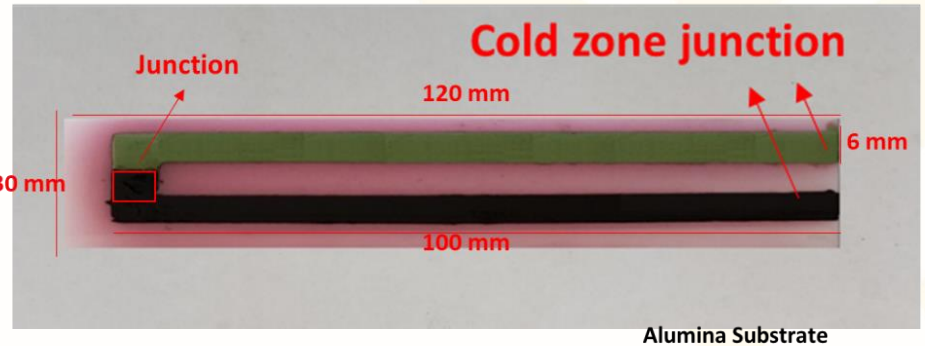

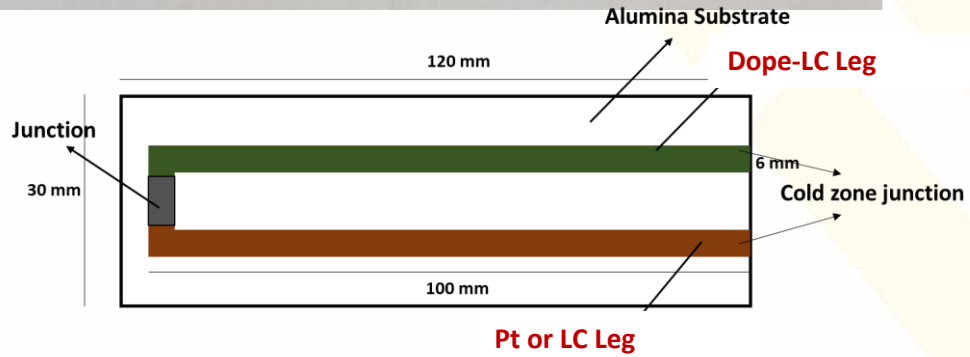

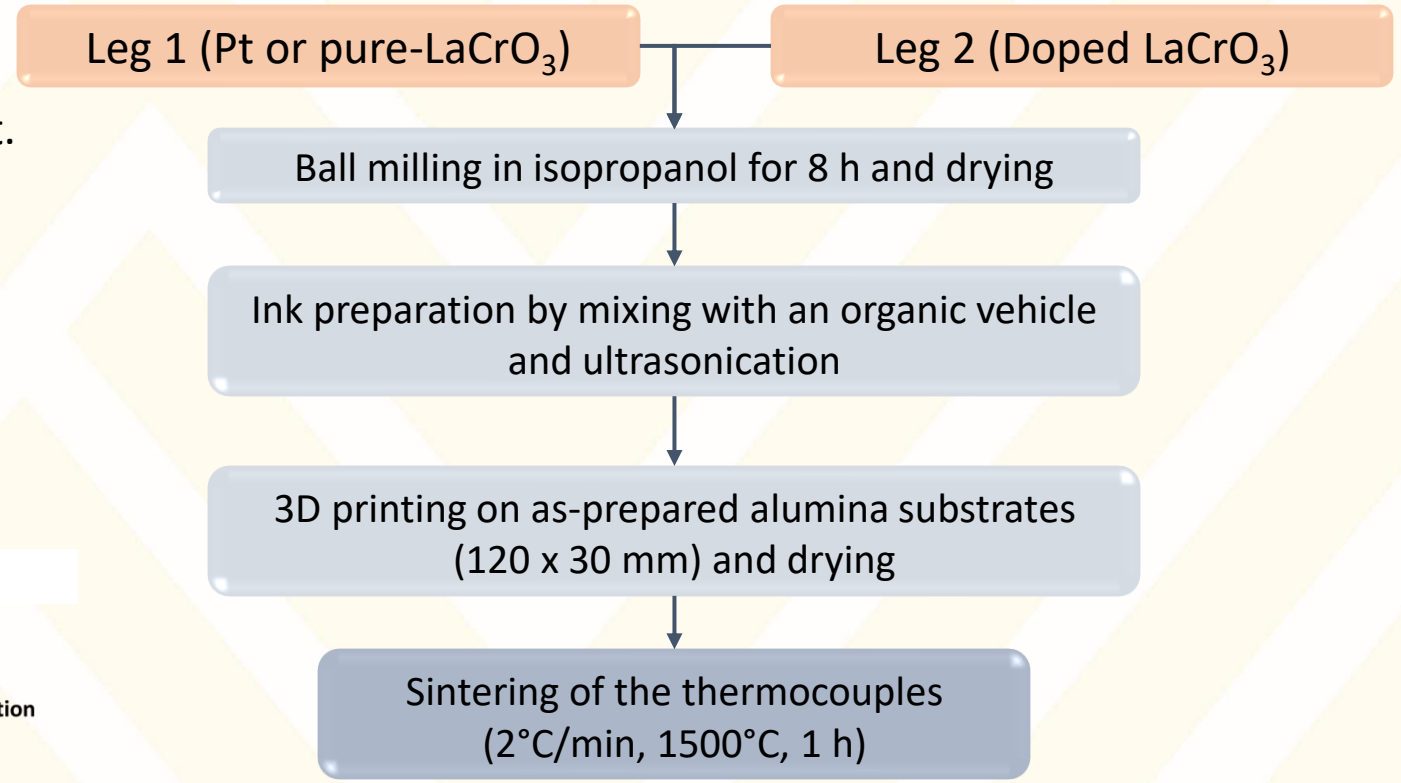

Seebeck Coefficient Estimation (Using Pt Standard)

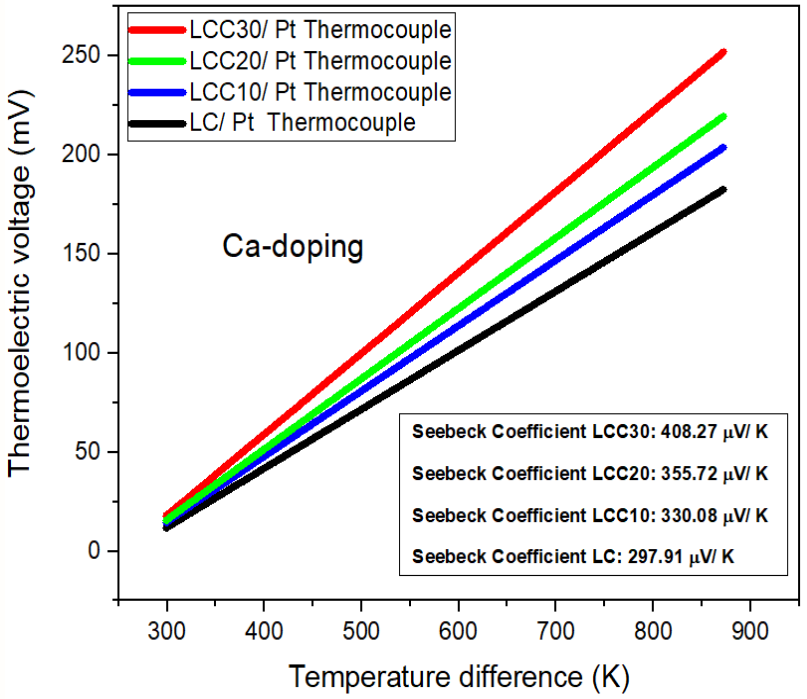

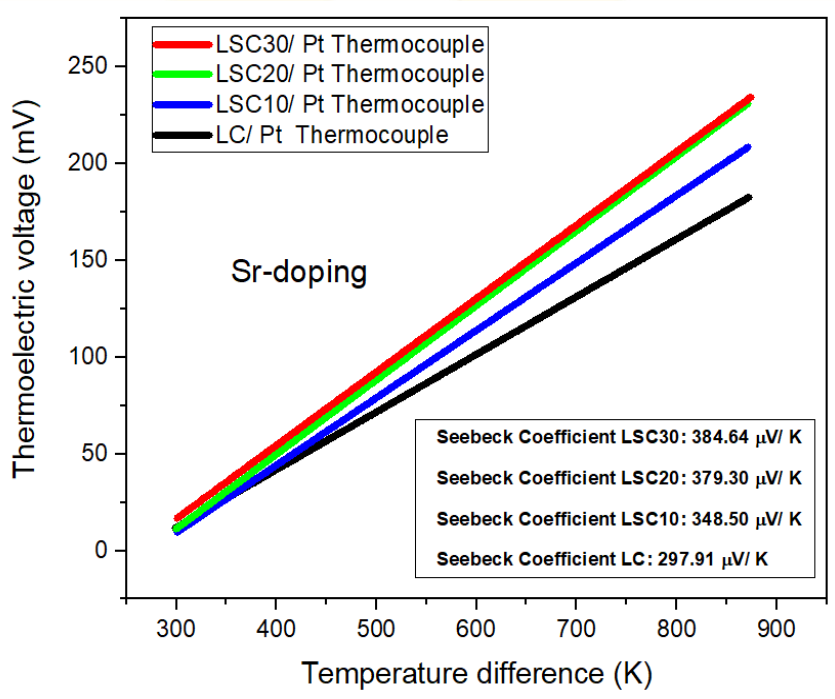

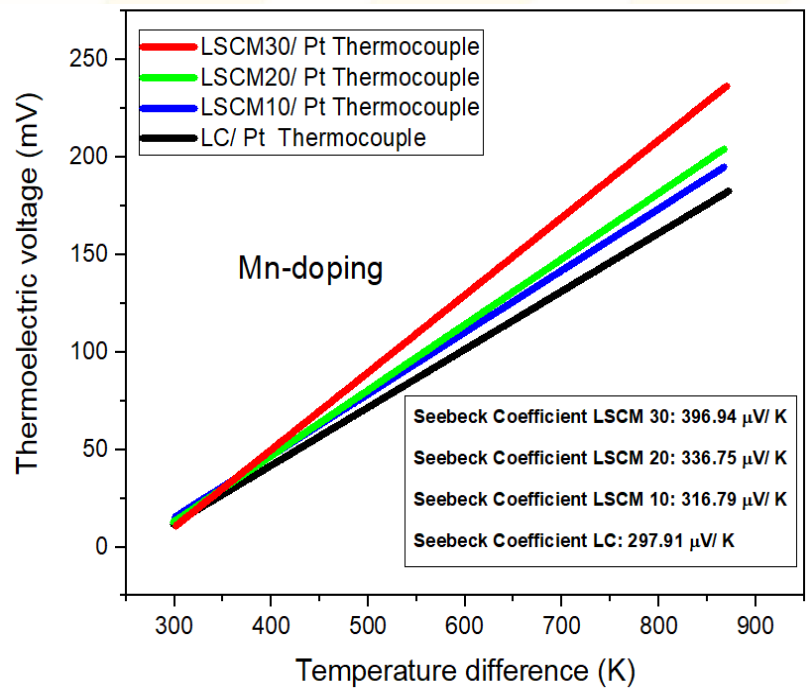

- Linear correlation between temperature difference and thermoelectric voltage was observed for all the compositions.
- Doped-$LaCrO_3$/Pt couples were fabricated to estimate absolute Seebeck coefficient (S_{Pt}~ -18 µV/K*) up to 1000°C.
- Ca doping shows highest absolute Seebeck coefficient (330-408 µV/K), with increasing Ca content.
- Ca doping on A-site has similar effect as Mn doping on B-site for LSC compositions.

*Moore, J. P. (1973). Journal of Applied Physics. 44 (3): 1174–1178

Thermoelectric Characterization of Thermocouples

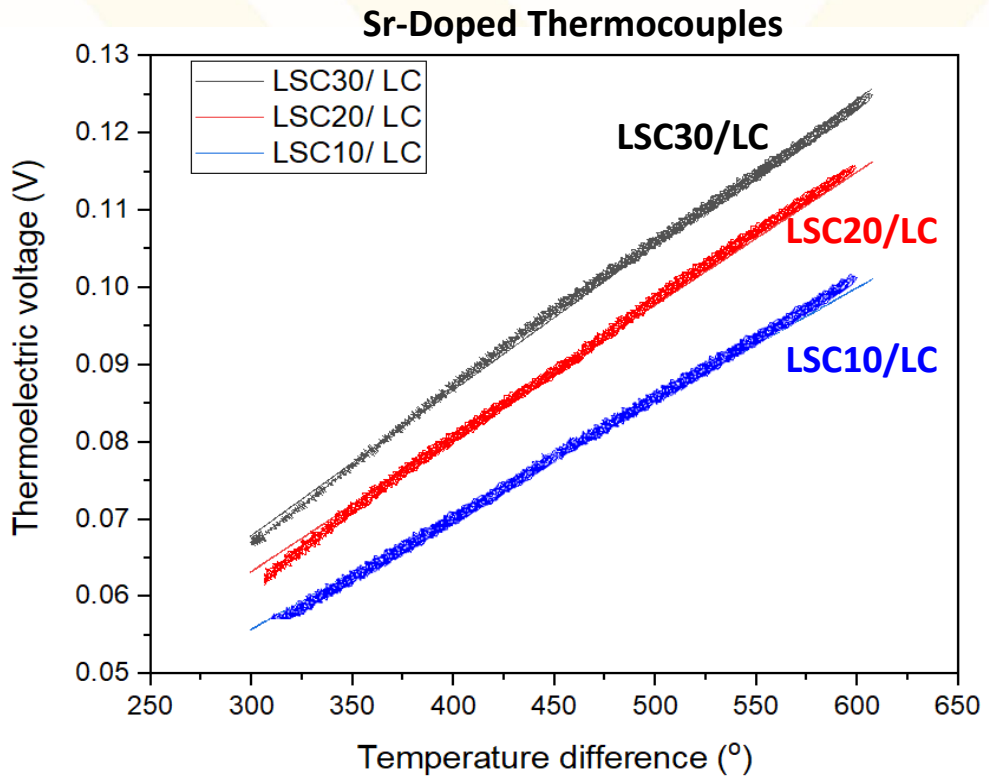

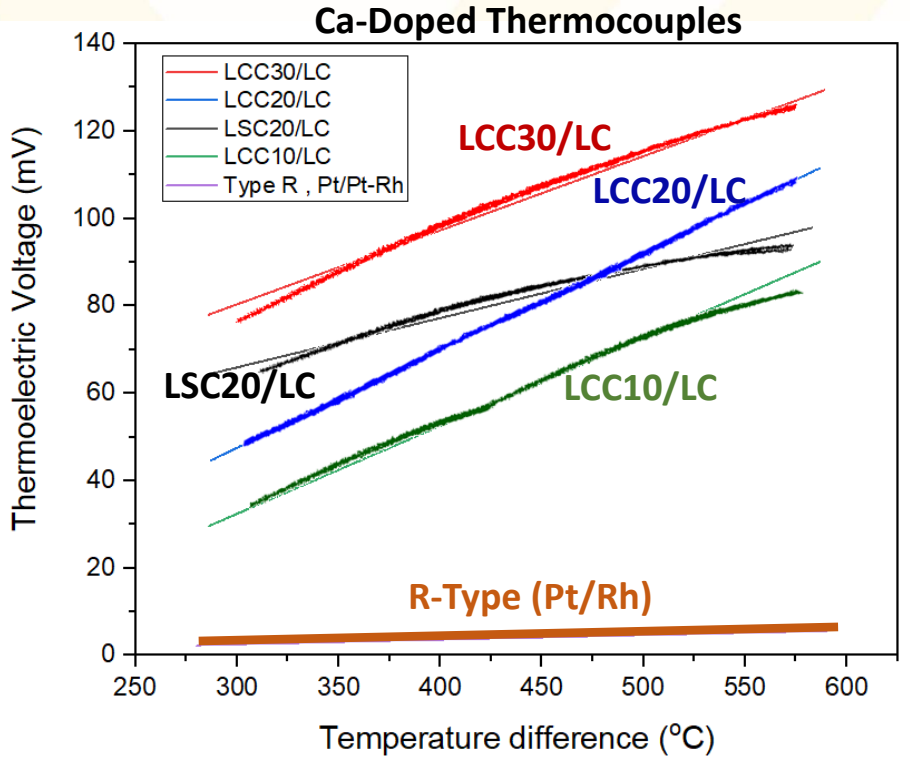

- Thermocouples were tested in a range between 30 to 750°C during 3 heating cycles, showing an excellent reproducibility.
- Sr-doped compositions have lower Seebeck coefficient over Ca-doped compositions.
- The LCC30/LC, LCC20/LC and LCC10/LC thermocouples showed a maximum higher voltage by **two orders of magnitude in comparison with Pt/Pt-Rh**, with values of 124.61 mV, 116.50 mV and 80 mV respectively (at ΔT~550°C).

Conclusions

- Using Pechini Sol-Gel method approach high density (~96%) doped lanthanum chromite compositions can be obtained. Uniform phase composition can be produced easily.

- Lattice parameters reduce proportionally with dopant content increment. Divalent dopants produce chromium oxidation state changes from +3 to +4 reducing the ionic radius.

- Electrical conductivity shows correlated dependence with high temperature (up to 1500^{o}C) for all compositions. The exponential Arrhenius trend is evidence for the polaron hopping electrical conduction mechanism.

Conclusions

- Conductivity increase in function of doping level up to 30% for all dopants (strontium, calcium and manganese).
- Under reducing conditions conductivity decrease, chromium changes oxidation state from +4 to +3 and oxygen vacancies form to keep neutrality.
- Doping increases Seebeck coefficient and permits functional thermocouples to be fabricated with pure $LaCrO_3$ (showing thermolelectric voltages 2× greater that Pt thermocouples).

Acknowledgment

❖We would like to thank U.S. Department of Energy (DOE) for sanctioning this project DE-FE0031825.

❖We also would like to acknowledge Mr. Harley Hart, Dr. Qiang Wang, and Dr. Marcela Redigolo for their cooperation and valuable assistance in the WVU Shared Facilities.

❖We also would like to thank HWI, for support us in developing real-life applications sensing systems/devices.

❖Kindly acknowledge faculty and staff of West Virginia University for their support.

Thank you for the attention.

Email:
ed.sabolsky@mail.wvu.edu